Low-Complexity Hybrid Adaptive Blind Equalization Algorithm for High-Order QAM Signals

Wei Rao[1, 2], Changlong Lu[3], Yuanyuan Liu[4], Jianqiu Zhang[1]
[1] Department of Electronic Engineering, Fudan University
Shanghai 200433, P. R. China
[e-mail: wrao14@fudan.edu.cn]
[2] School of Information Engineering, Nanchang Institute of Technology
Nanchang 330099, Jiangxi, P. R. China
[3] Department of electronic information engineering, Jingdezhen Ceramic Institute
Jingdezhen 333403, Jiangxi, P. R. China
[4] Faculty of information engineering, China University of Geoscience
Wuhan 430074, Hubei, P. R. China
*Corresponding author: Wei Rao

Received June 18, 2015; revised April 29, 2016; revised June 12, 2016; accepted July 11, 2016; published August 31, 2016

Abstract

It is well known that the constant modulus algorithm (CMA) presents a large steady-state mean-square error (MSE) for high-order quadrature amplitude modulation (QAM) signals. In this paper, we propose a low-complexity hybrid adaptive blind equalization algorithm, which augments the CMA error function with a novel constellation matched error (CME) term. The most attractive advantage of the proposed algorithm is that it is computationally simpler than concurrent CMA and soft decision-directed (SDD) scheme (CMA+SDD), and modified CMA (MCMA), while the approximation of steady-state MSE of the proposed algorithm is same with CMA+SDD, and lower than MCMA. Extensive simulations demonstrate the performance of the proposed algorithm.

Keywords: Blind Equalization, Constant Modulus Algorithm, Inter-Symbol Interference, Hybrid Algorithm, Low-Complexity

This research was supported by Natural Science Foundation of Jiangxi Province of China (Grant No. 2013ZBBE50016) and National Natural Science Foundation of China (Grant No. 61401188, No. 61571131).

http://dx.doi.org/10.3837/tiis.2016.08.019 **ISSN : 1976-7277**

1. Introduction

In the past, single-carrier communication was the modulation format of choice. In this context, inter-symbol interference (ISI) becomes the main factor affecting system performance. Recently, the orthogonal frequency division multiplexing (OFDM) protocol is being used in the transmission scheme for the majority of new communications systems. One of the most important advantages of OFDM systems is their robustness to multipath channels, thanks to the introduction of a cyclic prefix (CP), which efficiently combats ISI in time-dispersive channels. However, the insertion of a CP is pure redundancy, which decreases the spectral efficiency [1]. Additionally, when the CP length is shorter than the channel length, the effect of frequency-selective fading cannot be completely eliminated, and the intercarrier interference and ISI will be introduced. Blind equalization techniques without regular training/pilot symbols can be utilized to mitigate the problems [2, 3].

The constant modulus algorithm (CMA), pioneered by Godard [2], is by far the most popular blind equalization algorithm, since it can be easily implemented with good convergence properties [4]. For constant modulus signals, such as 4-QAM, a CMA-based fractionally spaced equalizer (FSE) can achieve a zero steady-state mean-square error (MSE) in noiseless channels. For non-constant modulus signals, such as high-order QAM signals which have been used for a long time in LTE mobile networks [5], it suffers a relatively large misadjustment resulting in a large steady-state MSE [4, 6].

A possible solution is to enable CMA until the eye diagram opens, and then switch to another adaptive equalization to minimize the residual error and compensate the phase offset. However, ensuring such a transfer is challenging, and sensitive to signal constellation, channel characteristics, and signal-to-noise (SNR) [7]. To this end, several soft-switching methods have been proposed. Weerackody et al. [8] provided a dual-mode type algorithm. In such an algorithm, the blind equalization mode works at higher error levels, while the mode similar to decision-direct (DD) works at lower error levels. De Castro et al. [7] suggested a typical low-complexity concurrent CMA and DD scheme (CMA+DD). Rather than switching to DD adaptation if CMA converges, they proposed enabling a DD equalizer concurrently with a CMA equalizer. The weight adaptation of DD equalizer follows that of CMA. To avoid error propagation due to incorrect decisions, the DD adjustment only works if the CMA adaptation is judged to be successful. At a cost of complexity, CMA+DD equalizer can obtain a dramatic performance improvement over CMA. To ease computational requirements in CMA+DD, Chen [9] proposed a concurrent CMA and soft DD scheme (CMA+SDD), wherein the soft DD part is an exponential weighted function of the distance between the equalizer soft output and the tentative decision. This soft decision enables a simultaneous update of both CMA and SDD weight vectors without error propagation. Compared with CMA+DD, CMA+SDD is reported to have simpler computational requirements, faster convergence rate and identical steady-state equalization performance. As a tradeoff, Xie et al. [10] proposed a concurrent dithered signed-error CMA (DSE-CMA) and SDD algorithm which can compensate the phase shift and provide better convergence and steady-state behavior than DSE-CMA while with less computation than CMA+SDD. Silva et al. [11] proposed a soft-switching blind equalization based on a convex combination of a blind equalization algorithm and a DD algorithm. The combination is adapted in a blind manner, and can automatically switch

between the component filters, avoiding MSE level settings a priori. Like CMA+SDD, this combination algorithm provides faster convergence rate and lower steady-state MSE than CMA+DD. Although its computational complexity was not clearly discussed, it still suffers high computation complexity because of the update of mixing parameters.

Recently, some hybrid blind equalization algorithms have attracted attention due to their relative simplicity and good performance. This hybrid approach, named constellation matched error (CME), combines CMA criterion with a penalty term, and with zero values at constellation points coordinates [12]. The most common CME functions encountered in the literature are polynomials of high order and powers of cosine functions [13, 14]. Afterwards, Thaiupathumpa et al. [15] added a CME to the cost function of generalized Sato algorithm [16]. He [17] added a CME to the cost function of multimodulus algorithm [18]. Sheikh and Fan [19] added a CME to the cost function of sliced multimodulus algorithm [20]. Labed et al. [21] introduced a CME, which is the product of $l1$-norm of the deviations of equalizer output from the constellation points [22].

In this paper, we propose a low-complexity hybrid adaptive blind equalization algorithm in which the hybrid cost function is a weighted sum of two separate well-defined error terms; one is identical to the CMA case, and the other is a new CME term based on a simple coordinate transformation. The approximation of the steady-state MSE of the proposed algorithm is derived, which is the same as that of the CMA+SDD [9] and lower than that of the modified CMA (MCMA) [14]. The most attractive advantage of the proposed algorithm is that, it is computationally simpler than CMA+SDD and MCMA. Extensive simulations demonstrate the performance of the proposed algorithm.

In Section 2, we review the blind equalization based on conventional CMA, CMA+SDD, and MCMA, respectively. In Section 3, a novel hybrid blind equalization algorithm is proposed. Section 4 addresses the computational complexity per weight update and the steady-state MSE analysis of the proposed algorithm. Section 5 presents simulation results in different situations. Finally, Section 6 provides the main conclusions of the paper.

2. Blind Equalization Using CMA, CMA+SDD, and MCMA

Equalization algorithms can be implemented in symbol-spaced form or fractionally spaced equalizer form (FSE). Here, we concentrate on fractionally spaced implementations due to their inherent advantages [23]. The schematic diagram of the T/2 FSE without channel noise is shown in **Fig. 1**. Given a fractionally spaced channel of finite length $2M$, the even and odd sets of channel coefficients can be collected into vectors as $\boldsymbol{c}_e = [c(0), c(2), \cdots, c(2M-2)]^T$ and $\boldsymbol{c}_o = [c(1), c(3), \cdots, c(2M-1)]^T$, respectively. Similarly, given a fractionally spaced equalizer of finite length $2N$, the even and odd sets of equalizer coefficients can be collected into vectors as $\boldsymbol{f}_e = [f(0), f(2), \cdots, f(2N-2)]^T$ and $\boldsymbol{f}_o = [f(1), f(3), \cdots, f(2N-1)]^T$, respectively.

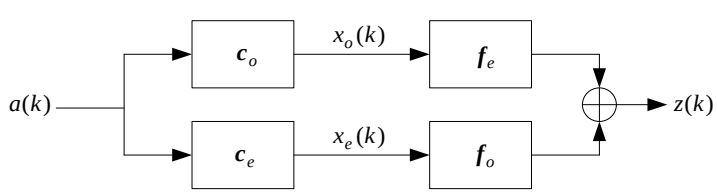

Fig. 1. Structure of $T/2$ FSE

A pair of $(M+N-1)\times N$ convolution matrices $\boldsymbol{C}_o$ and $\boldsymbol{C}_e$ are given by

$$\boldsymbol{C}_e=\begin{bmatrix} c(0) & & & \\ c(2) & c(0) & & \\ \vdots & c(2) & \ddots & \\ c(2M-2) & \vdots & \ddots & c(0) \\ & c(2M-2) & \ddots & c(2) \\ & & \ddots & \vdots \\ & & & c(2M-2) \end{bmatrix}, \boldsymbol{C}_o=\begin{bmatrix} c(1) & & & \\ c(3) & c(1) & & \\ \vdots & c(3) & \ddots & \\ c(2M-1) & \vdots & \ddots & c(1) \\ & c(2M-1) & \ddots & c(3) \\ & & \ddots & \vdots \\ & & & c(2M-1) \end{bmatrix} \tag{1}$$

We define the transmitted symbol vector as $\boldsymbol{a}_k=[a(k),a(k-1),\cdots,a(k-M-N+2)]$, and the compound matrix and vector quantities as

$$\boldsymbol{C}=[\boldsymbol{C}_o\ \boldsymbol{C}_e],\ \boldsymbol{f}=\begin{bmatrix}\boldsymbol{f}_e\\ \boldsymbol{f}_o\end{bmatrix} \tag{2}$$

Then, the output of the equalizer can be expressed as

$$z(k)=\boldsymbol{a}_k\boldsymbol{C}\boldsymbol{f} \tag{3}$$

In **Fig. 1**, $x_o(k)$ and $x_e(k)$ are the outputs of 2 sub-channels $\boldsymbol{c}_o$ and $\boldsymbol{c}_e$, respectively. Define $\boldsymbol{x}_{o,k}=[x_o(k),x_o(k-1),\cdots,x_o(k-N+1)]^T$ and $\boldsymbol{x}_{e,k}=[x_e(k),x_e(k-1),\cdots,x_e(k-N+1)]^T$, the input of the equalizer is thus given by

$$\boldsymbol{x}_k=\begin{bmatrix}\boldsymbol{x}_{o,k}\\ \boldsymbol{x}_{e,k}\end{bmatrix}=(\boldsymbol{a}_k\boldsymbol{C})^T \tag{4}$$

Then

$$z(k)=\boldsymbol{x}_k^T\boldsymbol{f} \tag{5}$$

2.1 CMA

In the T/2 FSE, the most popular adaptive blind equalization algorithm CMA2-2 [1] (CMA for simplicity) can be used to minimize a cost function defined by the CM criterion

$$J_{CM}(\boldsymbol{f})=\mathrm{E}[(|z(k)|^2-R)^2]/4 \tag{6}$$

where R is a fixed value of the transmitted sequence $\{a(\cdot)\}$ and defined as

$$R=\mathrm{E}[|a(k)|^4]/\mathrm{E}[|a(k)|^2] \tag{7}$$

CMA seeks to minimize the cost function (6) using stochastic gradient; hence, the

weight vector of the equalizer is updated by

$$\begin{cases} \boldsymbol{f}_{k+1} = \boldsymbol{f}_k + \mu \boldsymbol{x}_k^* e_o(k) \\ e_o(k) = z(k)[R - |z(k)|^2] \end{cases} \tag{8}$$

with a step-size μ. Here, the symbol * denotes complex conjugate transposition, and $e_o(k)$ denotes an instantaneous error.

Obviously, the CM criterion penalizes deviations in the modulus (i.e. magnitude) of the equalized signal $|z(k)|$ away from the fixed value $\sqrt{R}$. The CM criterion can successfully equalize signals characterized by source alphabets not possessing a constant modulus (e.g., 16-QAM), as well as those possessing a constant modulus (e.g., 4-QAM) (see **Fig. 2**). Unfortunately, toward non-constant modulus and constant modulus signals, CMA shows different performance.

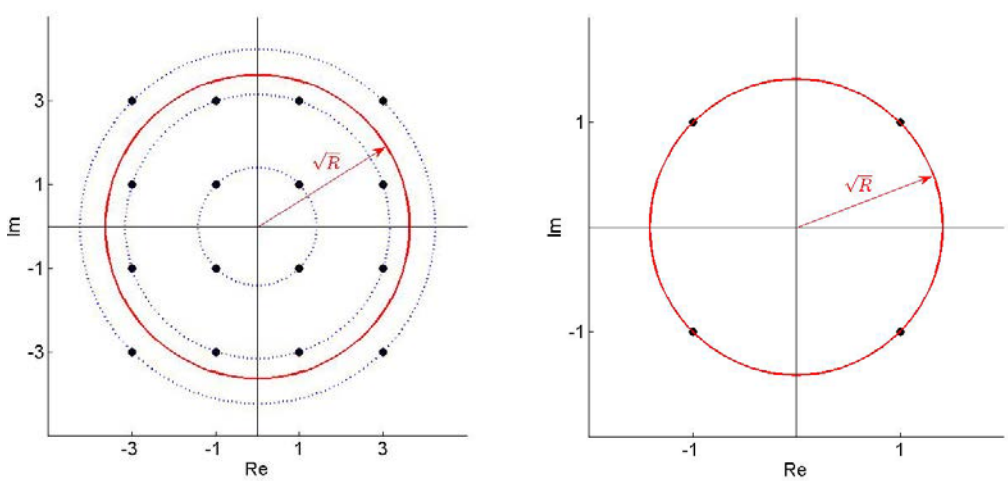

(a) (b)

Fig. 2. (a) Nonconstant modulus source constellation (16-QAM) versus (b) constant modulus source constellation (4-QAM).

For a constant modulus signal, a CMA-based FSE can achieve perfect equalization (i.e. $\mathrm{MSE} = 0$) in a noiseless environment. For example, for a 4-QAM constant modulus signal as shown in **Fig. 2(b)**, constellation points are $\{\pm 1 \pm j\}$ and $\sqrt{R} = \sqrt{2}$, if $z(k) = a(k)$ (i.e. $|z(k)| = \{\sqrt{2}\}$) in the steady state, then $e_o(k) = 0$ which terminates the updating of the weight vector, i.e., $\mathrm{MSE} = 0$.

For a non-constant modulus signal, a CMA-based FSE cannot achieve perfect equalization. For example, for a 16-QAM nonconstant modulus signal as shown in **Fig. 2(a)**, constellation points are $\{\pm 1 \pm j, \pm 1 \pm 3j, \pm 3 \pm j, \pm 3 \pm 3j\}$ and $\sqrt{R} = \sqrt{13.2}$, if $z(k) = a(k)$ (i.e. $|z(k)| = \{\sqrt{2}, \sqrt{10}, \sqrt{18}\}$) then $e_o(k) \neq 0$ which results in the weight vector keeps updating with a non-vanishing term and vibrates around the mean solution. Thus, $z(k) \neq a(k)$, i.e. $\mathrm{MSE} \neq 0$.

The steady-state MSE of CMA for the complex-valued cases can be approximated by [6]

$$\mathrm{MSE}_{\mathrm{CMA}} \approx \frac{\mu \mathrm{E}\{|a(k)|^6 - 2R|a(k)|^4 + R^2|a(k)|^2\}E\{\|\boldsymbol{x}_k\|^2\}}{2\mathrm{E}\{2|a(k)|^2 - R\}} \tag{9}$$

where $\mathrm{E}\{\|\boldsymbol{x}_k\|^2\}$ is the received signal norm.

2.2 CMA+SDD

Chen [9] proposed a blind equalization scheme consisting of a CMA equalizer and a SDD equalizer. The output of CMA+SDD is

$$z(k) = \boldsymbol{x}_k^T \boldsymbol{f}_c + \boldsymbol{x}_k^T \boldsymbol{f}_d \tag{10}$$

where $\boldsymbol{f}_c$ and $\boldsymbol{f}_d$ are the weight vectors with the same length $2N$ of the CMA equalizer and the SDD equalizer, respectively.

The CMA equalizer adjusts the weight vector $\boldsymbol{f}_c$ as (8)

$$\begin{cases} \boldsymbol{f}_{c,k+1} = \boldsymbol{f}_{c,k} + \mu \boldsymbol{x}_k^* e_{o,c}(k) \\ e_{o,c}(k) = z(k)[R - |z(k)|^2] \end{cases} \tag{11}$$

where μ is the step-size of the CMA equalizer.

The weight vector $\boldsymbol{f}_d$ of the SDD equalizer is updated by [9]

$$\begin{cases} \boldsymbol{f}_{d,k+1} = \boldsymbol{f}_{d,k} + \mu_d \boldsymbol{x}_k^* e_{o,d}(k) \\ e_{o,d}(k) = \dfrac{\sum_{p=2i-1}^{2i}\sum_{q=2l-1}^{2l}[a_{pq} - z(k)]e^{-\frac{|z(k)-a_{pq}|^2}{2\rho}}}{\sum_{p=2i-1}^{2i}\sum_{q=2l-1}^{2l} e^{-\frac{|z(k)-a_{pq}|^2}{2\rho}}}, \quad 1 \le i,l \le Q \end{cases} \tag{12}$$

where $Q = \sqrt{M} = 2^U$ and U is an integer, μ_d is the step-size of the SDD equalizer, and a_{pq} are four symbol points in a decision region which the equalizer output $z(k)$ belongs to. Typically, ρ is chosen to be <1.

Compared with CMA+DD, CMA+SDD blind equalizer has simpler computational requirements, faster convergence rate and identical steady-state equalization performance. For obtaining the approximate steady-state MSE of CMA+SDD, CMA+SDD is equivalent to the blind equalizer described by a hybrid cost function [24]. The two time evolution equations (11) and (12) are changed to be one time evolution with respect to one tap weight vector

$$\begin{cases} \boldsymbol{f}_{k+1} = \boldsymbol{f}_k + \mu \boldsymbol{x}_k^* e_o(k) \\ e_o(k) = z(k)[R - |z(k)|^2] + \alpha \dfrac{\sum\limits_{p=2i-1}^{2i} \sum\limits_{q=2l-1}^{2l} [a_{pq} - z(k)] e^{-\frac{|z(k)-a_{pq}|^2}{2\rho}}}{\sum\limits_{p=2i-1}^{2i} \sum\limits_{q=2l-1}^{2l} e^{-\frac{|z(k)-a_{pq}|^2}{2\rho}}} \end{cases} \tag{13}$$

where $\boldsymbol{f} = \boldsymbol{f}_c + \boldsymbol{f}_d$ and $\alpha = \mu_d / \mu$.

Now the steady-state MSE of CMA+SDD for the complex-valued cases can be approximated by [24]

$$\mathrm{MSE}_{\mathrm{CMA+SDD}} \approx \frac{\mu E\{|a(k)|^6 - 2R|a(k)|^4 + R^2|a(k)|^2\} E\{\|\boldsymbol{x}_k\|^2\}}{2E\{2|a(k)|^2 - R + \alpha\}} \tag{14}$$

2.3 MCMA

The Modified CMA (MCMA) [14] is the state-of-the-art hybrid method for the CMA, which augments the CMA error function with a constellation matched error (CME) term. The CME term provides MCMA with knowledge of the constellation allowing for faster convergence rate and greater reduction of MSE. The general form of the cost function for the MCMA is given by

$$J_{MCM}(\boldsymbol{f}) = \mathrm{E}\{(|z(k)|^2 - R)^2 / 4 + \beta[g(z_r(k)) + g(z_i(k))]\} \tag{15}$$

where the subscripts *r* and *i* correspond to the real and imaginary components, respectively, and β is the CME weighting factor. The weight vector of MCMA is updated by

$$\begin{cases} \boldsymbol{f}_{k+1} = \boldsymbol{f}_k + \mu \boldsymbol{x}_k^* e_o(k) \\ e_o(k) = z(k)[R - |z(k)|^2] + \beta \eta_k \end{cases} \tag{16}$$

where η_k is the CME term defined as [14]

$$\eta_k = \frac{d}{d\gamma} g(\gamma)\Big|_{\gamma = z_r(k)} + j \frac{d}{d\gamma} g(\gamma)\Big|_{\gamma = z_i(k)} \tag{17}$$

where $g(\gamma)$ is the CME function. The following CME function for QAM constellations is zero at symbol points [14]

$$g(\gamma) = 1 - \sin^{2n}(\gamma\pi / 2d) \tag{18}$$

where n is an integer number and $2d$ is the minimum distance between symbols. In this paper, d is set to be 1.

For $n=1$, the CME function is a cosine square, i.e. $g(\gamma)=\cos^2(\gamma\pi/2)$, as shown in **Fig. 3(a)**. In this case, it has the lowest complexity, and $e_o(k)$ in (16) is expressed as

$$e_o(k)=z(k)[R-|z(k)|^2]+\beta\frac{\pi}{2}\{\sin[z_r(k)\pi)]+j\sin[z_i(k)\pi)]\} \tag{19}$$

The difference between MCMA and CMA+SDD is that MCMA is based on one filter, while CMA+SDD has two filters. For CMA+SDD, its output is the sum of the output of the two filters, which operates under two cost functions. The MCMA equalizer, on the other hand, has one filter, whose weight vector is updated according to one cost function, which includes both CMA and CME terms. While in [24], the CMA+SDD blind equalizer can be equivalent to the blind equalizer described by a hybrid cost function, whose SDD part can be set to be a CME term, as shown in (13).

For $n=1$ and $d=1$, the steady-state MSE of MCMA can be approximated by [14]

$$\mathrm{MSE}_{\mathrm{MCMA}}\approx \frac{\mu E\{|a(k)|^6-2R|a(k)|^4+R^2|a(k)|^2\}E\{\|\boldsymbol{x}_k\|^2\}}{2E\{2|a(k)|^2-R+\frac{\pi^2\beta}{2}\}-\mu E\{\|\boldsymbol{x}_k\|^2[9|a(k)|^4+4(\frac{\pi^2\beta}{2}-2R)|a(k)|^2+(\frac{\pi^2\beta}{2}-R)]\}} \tag{20}$$

where $\pi^2\beta/2$ is usually larger than $2R$.

3. Proposed Algorithm

3.1 The CME term of the proposed algorithm

In our algorithm, construction of the CME term according to the transmitted symbol characteristics is the key to improve algorithm performance. We assume a transmitted symbol a has coordinates (a_r,a_i), i.e. $a=a_r+ja_i$, in a constellation diagram. For M-QAM, we have

$$\begin{cases}a_r=2g-2^L-1\\ a_i=2h-2^L-1\end{cases},\ 1\le g,h\le 2^L,\ M=2^{2L},\ L\ge 1 \tag{21}$$

where g, h, and L are integers, and the minimum distance between symbol points is set to be 2 (as shown in **Fig. 2**) for simplicity. For high-order QAM signals, $L\ge 2$.

To form the CME term of the proposed algorithm, we firstly introduce a coordinate transformation criterion

$$\begin{cases}\chi_{n,r}=\chi_{n-1,r}-2^{L-n}\,\mathrm{sgn}(\chi_{n-1,r})\\ \chi_{n,i}=\chi_{n-1,i}-2^{L-n}\,\mathrm{sgn}(\chi_{n-1,i})\end{cases},\ 1\le n\le L-1,\ L\ge 2 \tag{22}$$

where $\mathrm{sgn}(\cdot)$ is a sign function, n is an integer between 1 and $L-1$, and χ_{L-1} is the new

coordinate transformed from the original coordinate χ_0 by using (22).

In (22), let $\chi_{0,r} = a_r$ and $\chi_{0,i} = a_i$, then $\chi_{L-1,r}$ and $\chi_{L-1,i}$ can be obtained as s_r and s_i, respectively. Then the process of change for different high-order M-QAM signals can be described as follows.

1) For a 16-QAM signal ($L=2$) with $a_r = a_i = \{\pm 1, \pm 3\}$,

$$\begin{cases} s_r = a_r - 2\mathrm{sgn}(a_r) = 1 \text{ or } -1 \\ s_i = a_i - 2\mathrm{sgn}(a_i) = 1 \text{ or } -1 \end{cases} \tag{23}$$

2) For a 64-QAM signal ($L=3$) with $a_r = a_i = \{\pm 1, \pm 3, \pm 5, \pm 7\}$,

$$\begin{cases} s_r = a_r - 4\mathrm{sgn}(a_r) - 2\mathrm{sgn}[a_r - 4\mathrm{sgn}(a_r)] = 1 \text{ or } -1 \\ s_i = a_i - 4\mathrm{sgn}(a_i) - 2\mathrm{sgn}[a_i - 4\mathrm{sgn}(a_i)] = 1 \text{ or } -1 \end{cases} \tag{24}$$

3) For a 256-QAM signal ($L=4$) with $a_r = a_i = \{\pm 1, \pm 3, \pm 5, \pm 7, \pm 9, \pm 11, \pm 13, \pm 15\}$,

$$\begin{cases} s_r = a_r - 8\mathrm{sgn}(a_r) - 4\mathrm{sgn}[a_r - 8\mathrm{sgn}(a_r)] - 2\mathrm{sgn}\{a_r - 8\mathrm{sgn}(a_r) - 4\mathrm{sgn}[a_r - 8\mathrm{sgn}(a_r)]\} = 1 \text{ or } -1 \\ s_i = a_i - 8\mathrm{sgn}(a_i) - 4\mathrm{sgn}[a_i - 8\mathrm{sgn}(a_i)] - 2\mathrm{sgn}\{a_i - 8\mathrm{sgn}(a_i) - 4\mathrm{sgn}[a_i - 8\mathrm{sgn}(a_i)]\} = 1 \text{ or } -1 \end{cases} \tag{25}$$

It is clear that the following functions take zero values at every symbol point of high-order M-QAM signals by using the coordinate transformation criterion

$$\begin{cases} s_r - \mathrm{sgn}(s_r) \\ s_i - \mathrm{sgn}(s_i) \end{cases} \tag{26}$$

For the equalizer output signal ($z = z_r + jz_i$), let $\chi_{0,r} = z_r$ and $\chi_{0,i} = z_i$ in (22), then $\chi_{L-1,r}$ and $\chi_{L-1,i}$ are obtained as y_r and y_i respectively,

$$\begin{cases} y_r - \mathrm{sgn}(y_r) = 0 \\ y_i - \mathrm{sgn}(y_i) = 0 \end{cases} \tag{27}$$

when the output signals are the same as the transmitted signals.

So the CME function of the proposed algorithm is given by

$$g(\chi) = [\chi_{L-1} - \mathrm{sgn}(\chi_{L-1})]^2 \tag{28}$$

Take a 16-QAM signal for example, from (23) and (28) the CME function of the proposed algorithm, as shown in **Fig. 3(b)**, is

$$g(\chi) = \{[\chi - 2\mathrm{sgn}(\chi)] - \mathrm{sgn}[\chi - 2\mathrm{sgn}(\chi)]\}^2 \tag{29}$$

From **Fig. 3(b)**, the CME function (29) of the proposed algorithm satisfies the following

properties.

1) The function is symmetric with respect to each alphabet when $-4 \le \chi \le 4$.

2) The minimum values are zeros and only occur at the constellation points ± 1 and ± 3. If the equalizer output is near the constellation points, it has a local maximum 0.5 which is reached at the center points between two consecutive alphabets. If the equalizer output is far away from the constellation points, i.e., $|\chi| > 4$, the function will place the higher penalty.

With property 2), the proposed algorithm can provide better performance than MCMA, since the minimum values of MCMA's CME function occur not only at the constellation points but also at the unexpected position, as shown in **Fig. 3(a)**. For instance, for a 16-QAM signal with constellation points ± 1 and ± 3, if the received signal is far away from the constellation points, then this signal is equalized to ± 5 (even ± 7) by the CME function of the MCMA, since at these points the values of the CME function are also zeros. So the CME function of the proposed algorithm has lower misadjustment than that of the MCMA, which means the proposed algorithm can obtain better convergence performance.

From (17) and (28), we get the CME term of the proposed algorithm

$$\eta_k = y_r(k) - \mathrm{sgn}[y_r(k)] + j\{y_i(k) - \mathrm{sgn}[y_i(k)]\} \tag{30}$$

where $y_r(k)$ and $y_i(k)$ are derived from $z_r(k)$ and $z_i(k)$ by using (22), respectively.

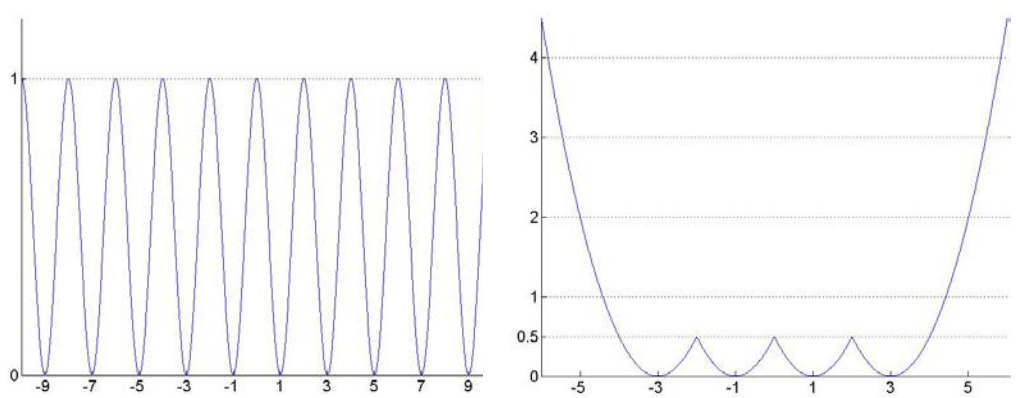

(a) (b)

Fig. 3. The CME functions of MCMA (a) and proposed algorithm (b) for the 16-QAM signal.

3.2 Proposed algorithm

The general form of the cost function of the proposed algorithm is given by

$$J_{NEW}(\boldsymbol{f}) = E\{\frac{1}{4}[|z(k)|^2 - R]^2 + \frac{1}{2}\lambda\{\{y_r(k) - \mathrm{sgn}[y_r(k)]\}^2 + \{y_i(k) - \mathrm{sgn}[y_i(k)]\}^2\}\} \tag{31}$$

The weight vector of the proposed algorithm is updated by

$$\begin{cases} \boldsymbol{f}_{k+1} = \boldsymbol{f}_k + \mu \boldsymbol{x}_k^* e_o(k) \\ e_o(k) = z(k)[R - |z(k)|^2] - \lambda\{y_r(k) - \mathrm{sgn}[y_r(k)] + j\{y_i(k) - \mathrm{sgn}[y_i(k)]\}\} \end{cases} \tag{32}$$

Like the MCMA, the weighting factor λ in (32) trades off amplitude and constellation-matched errors. Large λ increases convergence time, whereas small λ diminishes the advantage of CME in reducing the steady-state residual errors. Accordingly, λ is chosen to satisfy [14]

$$\lambda | y_r(k) - \mathrm{sgn}[y_r(k)] + j\{y_i(k) - \mathrm{sgn}[y_i(k)]\} |_{\max} < \max_{a \in alphabet} | a(|a|^2 - R) | \tag{33}$$

The CME function of the proposed algorithm only has a local maximum 0.5, so in (33) the local maximum is used. It cannot affect the performance of the proposed algorithm because when the equalizer output is far away from the constellation points, the CME function places the right higher penalty, i.e. enforces it to be close to the constellation points. The above equation translates to $\lambda < 57.6$ for 16-QAM, $\lambda < 1120.2$ for 64-QAM, and $\lambda < 12770$ for 256-QAM, respectively.

4. Performance Analysis

In this section, we show the complexity of the proposed algorithm. Without loss of generality, we derive an analytical expression for the steady-state MSE of the proposed algorithm for 16-QAM in a noiseless environment.

4.1 Computational complexity

The computational requirements of the proposed algorithm (for 16-QAM), CMA, CMA+SDD, and MCMA are summarized in **Table 1**. And the computational requirements of the proposed algorithm for different high-order M-QAM signals are shown in **Table 2**. From **Table 1**, CMA+SDD requires $12 \times 2N + 29$ multiplications, $14 \times 2N + 21$ additions and 4 exponential operations for each iteration, which indicates a higher complexity than that of CMA. Therefore, CMA+SDD obtains a dramatic performance improvement over CMA at a cost of complexity. The proposed algorithm requires $8 \times 2N + 10$ multiplications and $8 \times 2N + 6$ additions and 4 sign operations for each iteration. It has the similar computational complexity to CMA. So, compared with the CMA+SDD, a considerable computational saving is obtained by the proposed algorithm. Moreover, the MCMA equalizer for calculating the sine function may be balanced for constraints such as speed, accuracy, portability, or range of accepted input values. Hence the computational complexity of the proposed algorithm is also simpler than that of the MCMA.

4.2 Steady-state MSE Performance

Without loss of generality, for the 16-QAM signal we derive the steady-state MSE performance of the proposed algorithm without noise using the method proposed in [6]. The key formula for evaluating the steady-state MSE of the adaptive algorithm is [6]

$$\mathrm{E}\left\{\frac{|e_a(k)|^2}{\|\boldsymbol{x}(k)\|^2}\right\}=\mathrm{E}\left\{\frac{|e_a(k)|^2}{\|\boldsymbol{x}(k)\|^2}\right\}-\underbrace{\mu\mathrm{E}\{[e_a(k)e_o^*(k)+e_a^*(k)e_o(k)]\}}_{T_1}+\underbrace{\mu^2\mathrm{E}\{\|\boldsymbol{x}(k)\|^2|e_o(k)|^2\}}_{T_2} \quad (34)$$

This implies that the terms T_1 and T_2 are identical. From this equality, we can obtain an approximate expression for the steady-state MSE $\mathrm{E}\{|e_a(k)|^2\}$. And $e_a(k)$ is defined as

$$e_a(k)=a(k)-z(k) \quad (35)$$

Table 1. Comparison of computational complexity per weight update

Equalizer	Multiplications	Additions	exp(.) evaluations	sgn(.) evaluations	sin(.) evaluations
CMA	$8\times 2N+6$	$8\times 2N$	-	-	-
CAM+SDD	$12\times 2N+29$	$14\times 2N+21$	4	-	-
MCMA	$8\times 2N+12$	$8\times 2N+2$	-	-	2
Proposed algorithm	$8\times 2N+10$	$8\times 2N+6$	-	4	-

Table 2. The computational requirements of the proposed algorithm per weight update for different high-order M-QAM signals

M-QAM	Multiplications	Additions	sgn(.) evaluations
16-QAM	$8\times 2N+10$	$8\times 2N+6$	4
64-QAM	$8\times 2N+12$	$8\times 2N+8$	6
256-QAM	$8\times 2N+14$	$8\times 2N+10$	8

The $e_o(k)$ of the proposed algorithm is in (32)

$$e_o(k)=z(k)[R-|z(k)|^2]-\lambda\{y_r(k)-\mathrm{sgn}[y_r(k)]+j\{y_i(k)-\mathrm{sgn}[y_i(k)]\}\} \quad (36)$$

where $y_r(k)=z_r(k)-2\mathrm{sgn}[z_r(k)]$ and $y_i(k)=z_i(k)-2\mathrm{sgn}[z_i(k)]$ for the 16-QAM signal.

For the 16-QAM signal, $s_r(k)=a_r(k)-2\mathrm{sgn}[a_r(k)]=\{\pm 1\}$ and $s_i(k)=a_i(k)-2\mathrm{sgn}[a_i(k)]=\{\pm 1\}$. And in the steady state, $\mathrm{sgn}[y_r(k)]=\mathrm{sgn}[s_r(k)]=s_r(k)$, $\mathrm{sgn}[y_i(k)]=\mathrm{sgn}[s_i(k)]=s_i(k)$, $\mathrm{sgn}[z_r(k)]=\mathrm{sgn}[a_r(k)]$, and $\mathrm{sgn}[z_i(k)]=\mathrm{sgn}[a_i(k)]$. So in steady state the $e_o(k)$ can be rewritten as

$$e_o(k)=z(k)[R-|z(k)|^2]+\lambda e_a(k) \quad (37)$$

The analysis that follows for the proposed algorithm is based on the assumptions made in [6] regarding the independence of the transmitted symbol $a(k)$ and $e_a(k)$, and the independence of $\mu^2\|\boldsymbol{x}(k)\|^2$ and the equalizer output $z(k)$. Furthermore, we can conclude the independence of $s(k)$ and $e_a(k)$, and the independence of $\mu^2\|\boldsymbol{x}(k)\|^2$ and $y(k)$. In addition, we drop the time index k for simplicity and assume the step-size μ is sufficiently small and the value $|e_a(k)|^2$ is reasonably small in steady state.

For T_1, we obtain

$$T_1 = \underbrace{\mu E\{e_a^* z(R-|z|^2) + e_a z^*(R-|z|^2)\}}_{A} + \lambda\mu E\{e_a^* e_a + e_a e_a^*\} \tag{38}$$

The term A can be approximated by $2\mu E(2|a|^2 - R)E\{|e_a|^2\}$ as shown in [6]. Then

$$T_1 \approx 2\mu E(2|a|^2 - R + \lambda)E\{|e_a|^2\} \tag{39}$$

For T_2, we obtain

$$T_2 = \underbrace{\mu^2 E\{\|\boldsymbol{x}\|^2 |z(R-|z|^2)|^2\}}_{B} + \underbrace{\lambda^2\mu^2 E\{\|\boldsymbol{x}\|^2 |e_a|^2\}}_{D} + \underbrace{\lambda\mu^2 E\{\|\boldsymbol{x}\|^2 [z(R-|z|^2)e_a^* + e_a z^*(R-|z|^2)]\}}_{F} \tag{40}$$

The term B can be approximated by $\mu^2 E\{|a|^6 - 2R|a|^4 + R^2|a|^2\}E\{\|\boldsymbol{x}\|^2\}$ as shown in [3]. The term D can be neglected for small μ and small $|e_a|$. By substituting z by $a - e_a$, we get

$$F = \lambda\mu^2 E\{\|\boldsymbol{x}\|^2 [(e_a a^* - 2|e_a|^2 + a e_a^*)][R - (|a|^2 - a^* e_a - a e_a^* + |e_a|^2)]\} \tag{41}$$

By expanding F and neglecting the terms containing $\mu^2|e_a|^2$ for some μ and small $|e_a|$ and using the independence of a and e_a, we obtain the approximation $F \approx 0$. Now we have

$$T_2 \approx \mu^2 E\{|a|^6 - 2R|a|^4 + R^2|a|^2\}E\{\|\boldsymbol{x}\|^2\} \tag{42}$$

From the equality $T_1 = T_2$, the steady-state MSE of proposed algorithm can be approximated by

$$E\{|e_a|^2\} \approx \frac{\mu E\{|a|^6 - 2R|a|^4 + R^2|a|^2\}E\|\boldsymbol{x}\|^2}{2E\{2|a|^2 - R + \lambda\}} \tag{43}$$

Similarly, the steady-state MSE expressions for 64-QAM and 256-QAM can be calculated, which are the same as the equation (43).

It is clear that when the weighting factor λ is zero, equation (43) is identical with the steady-state MSE of the conventional stochastic gradient descent CMA as shown in (9). The steady-state MSE of the proposed algorithm is linearly proportional to the step-size μ and the received signal norm $E\|\boldsymbol{x}\|^2$. In steady state, the weighting factor λ only exits in the denominators of (43), and the MSE will decrease with the increase of λ.

It is important to note that the MSE expressions of CMA (9), CMA+SDD (14), MCMA (20) and proposed algorithm (43) have the same numerator. Therefore, the relationships between them depend on the denominators. Specifically,

1) $\mathrm{MSE}_{\mathrm{CMA+SDD}} < \mathrm{MSE}_{\mathrm{CMA}}$, since $\alpha = \mu_d / \mu > 0$.

2) $\mathrm{MSE}_{\text{Proposed algorithm}} < \mathrm{MSE}_{\text{CMA}}$, since $\lambda > 0$.

3) $\mathrm{MSE}_{\text{Proposed algorithm}} \approx \mathrm{MSE}_{\text{CMA+SDD}}$, when $\lambda = \alpha$.

4) $\mathrm{MSE}_{\text{Proposed algorithm}} \approx \mathrm{MSE}_{\text{CMA+SDD}} > \mathrm{MSE}_{\text{MCMA}} > \mathrm{MSE}_{\text{CMA}}$, when $\lambda = \alpha = \pi^2\beta/2$.

5. Simulation Results

Firstly, we provide simulation results that compare the experimental performance with the one predicted by the analysis in this section. In this simulation, the transmitted data symbols are 16-QAM, 64-QAM and 256-QAM, respectively. The channel considered in this simulation is given by $\boldsymbol{c}_1 = [0.1, 0.3, 1, -0.1, 0.5, 0.2]^T$ [6]. A 10-tap FIR filter is used as a *T*/2-FSE. Under different step-size μ (from 3×10^{-5} to 5×10^{-5}) with fixed weighting factor $\lambda = 20$ and $\lambda = 50$, respectively, **Fig. 4(a)** shows two groups of curves for the experimental results of the steady-state MSE and the theoretical results of (43) for 16-QAM. Under different weighting factor λ (from 0 to 50) with fixed step-size $\mu = 3\times10^{-5}$ and $\mu = 4\times10^{-5}$, respectively, **Fig. 4(b)** shows two groups of curves for the experimental results of the steady-state MSE and theoretical results of (43) for 16-QAM. From these two figures, we can observe that two steady-state MSEs are matched reasonably well, and linearly proportional to the step-size μ, and increase with decreasing λ. The similar simulation results for 64-QAM and 256-QAM are shown in **Fig. 5** and **Fig. 6**, respectively.

Secondly, the performance of discussed blind equalization algorithms for 64-QAM are compared. Additionally, to illustrate the advantage of the proposed algorithm we consider the constant norm algorithm (CNA) proposed in [25], which has proven to be particularly adapted to square constellations. Since we pay more attention to the CMA+SDD [9], the same simulation parameters described in [9] are considered. The channel $\boldsymbol{c}_2$ in [9, Table 2] is used and the parameters of the algorithms are set as follows: *N*= 11 and $\mu = 5\times10^{-7}$ for every algorithm, $\lambda = 400$ for the proposed algorithm, $\alpha = \lambda$ and $\rho = 0.6$ for the CMA+SDD, and $\beta = 2\lambda/\pi^2$ for the MCMA. **Fig. 7** shows the simulation results for four different SNRs. The MSE traces of these algorithms shown in **Fig. 7** verify that the proposed algorithm and the CMA+SDD have the similar steady-state MSE and convergence rate which are better than those of CMA, CNA and MCMA. Although in the case of lower SNR the steady-state MSE of the proposed algorithm is not much lower than that of the MCMA, the convergence rate of the proposed algorithm is much faster than that of the MCMA. It is interesting to note that the advantages of the proposed algorithm are more significant in higher SNR.

Finally, we compare the performance of discussed blind equalization algorithms through two different channels for 256-QAM. From n=0 to n=40000, we consider the cable channel $\boldsymbol{c}_3$ from the signal processing information base (SPIB, located at http://spib.rice.edu/) and at n=40000, it is changed abruptly to channel $\boldsymbol{c}_4 = [0.36\ 0.86\ 0.36]^T$ [26]. In both cases, the remaining parameters of the algorithms are set as follows: *N*= 21 and $\mu = 10^{-8}$ for every algorithm, $\lambda = 1800$ for the proposed algorithm, $\alpha = \lambda$ and $\rho = 0.7$ for the CMA+SDD, and $\beta = 2\lambda/\pi^2$ for MCMA. Additionally, we do not consider CNA in this simulation since the CNA is very suitable for high-order QAM constellation but not including 256-QAM

[25]. In practice, CMA achieves better performance than CNA for 256-QAM. The learning curves of these algorithms are depicted in **Fig. 8**. We can observe that the proposed algorithm has the lowest steady-state MSE, and the fast convergence rate as CMA+SDD even in the variable channels.

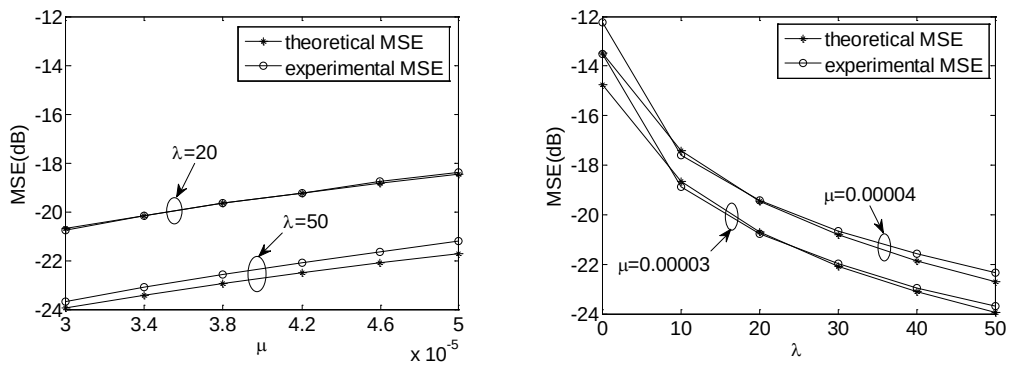

Fig. 4. Theoretical and experimental steady-state MSE curves against step-size μ (a) and weighting factor λ (b) in a noise free environment for 16-QAM signal and channel $\boldsymbol{c}_1$.

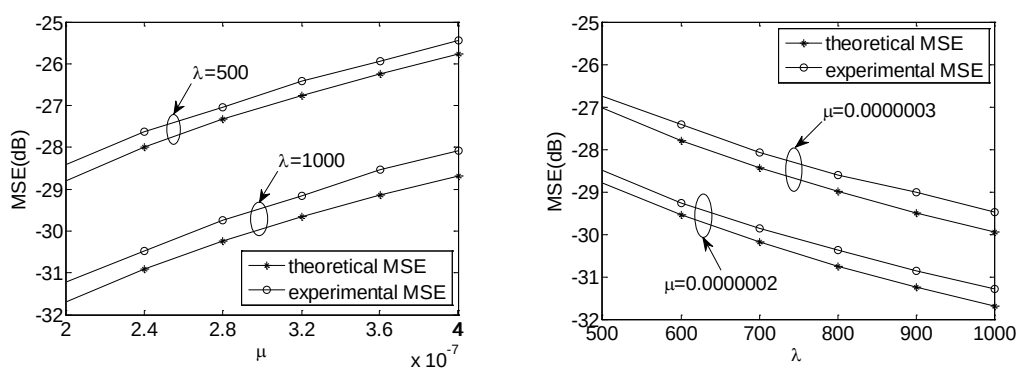

Fig. 5. Theoretical and experimental steady-state MSE curves against step-size μ (a) and weighting factor λ (b) in noise free environment for 64-QAM signal and channel $\boldsymbol{c}_1$.

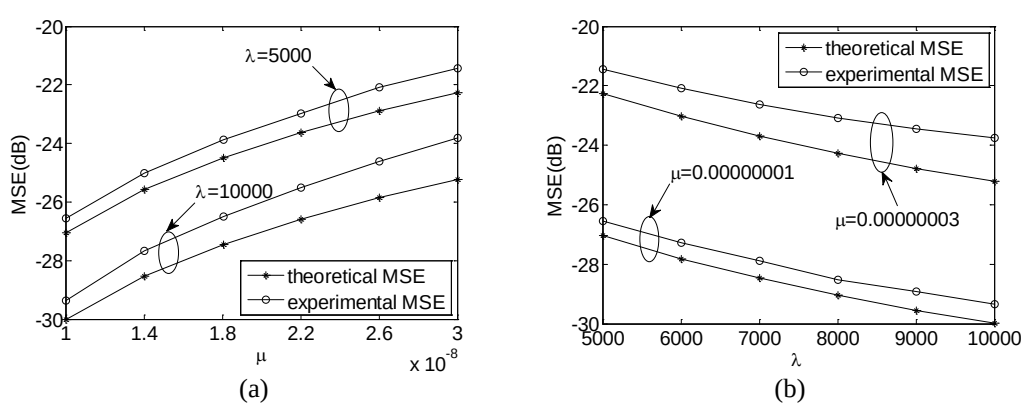

Fig. 6. Theoretical and experimental steady-state MSE curves against step-size μ (a) and weighting factor λ (b) in noise free environment for 256-QAM signal and channel $\boldsymbol{c}_1$.

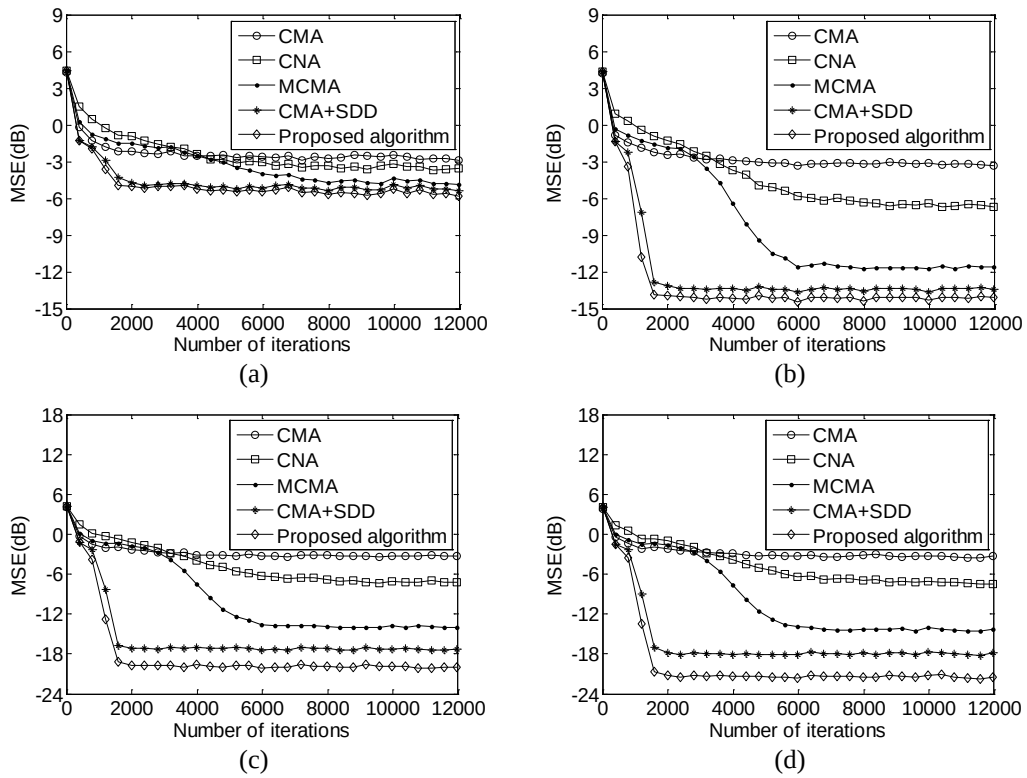

Fig. 7. Performance comparison of CMA, CNA, MCMA, CMA+SDD, and proposed algorithm for 64-QAM and channel $\boldsymbol{c}_2$ with different SNR values. (a) SNR=20dB. (b) SNR=30 dB. (c) SNR= 40dB. (d) SNR=50 dB.

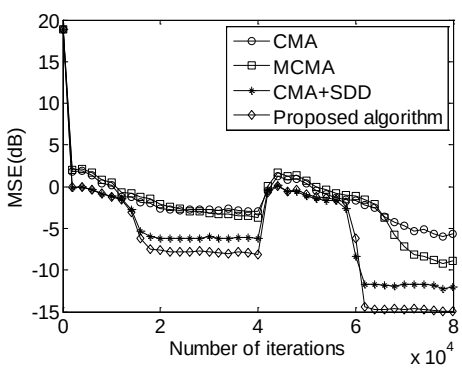

Fig. 8. MSE traces for CMA, MCMA, CMA+SDD, and proposed algorithm for 256-QAM through channels $\boldsymbol{c}_3$ and $\boldsymbol{c}_4$.

6. Conclusions

In this paper, we studied a novel low-complexity hybrid blind equalization algorithm that minimizes a cost function made up of CMA and coordinate transformation-based CME terms. The steady-state performance analysis of the proposed technique was developed. The proposed algorithm has a significantly lower computational complexity than the CMA+SDD, and has the same steady-state performance as the CMA+SDD. When

compared with the MCMA, the proposed algorithm has lower computational complexity, lower steady-state MSE and faster convergence rate. Simulation results for 16-QAM, 64-QAM, and 256-QAM confirm the effectiveness of the new blind algorithm over existing CMA, CAN, CMA+SDD, and MCMA.

In future work, we will consider applying the proposed algorithm instead of CNA in [27] to improve the performance of blind equation used into OFDM/OQAM. In addition, we will find a way to combine the linear programming technique with the proposed blind equalization to further improve the performance, since the recent research of linear programming applied to blind equalization has proved a significant advance [28].

References

[1] T. Fusco, L. Izzo, A. Petrella and M. Tanda, "Blind Symbol Timing Estimation for OFDM/OQAM Systems," *IEEE Transactions on Signal Processing*, Vol. 57, No. 12, pp. 4952-2958, 2009. Article (CrossRef Link)

[2] D. N. Godard, "Self-recovering equalization and carrier tracking in two dimensional data communication systems," *IEEE Transactions on Communications*, Vol. 28, No. 11, pp. 1867-1875, 1980. Article (CrossRef Link)

[3] R.K. Martin, C.R. Johnson, "Adaptive equalization: transitioning from single-carrier to multicarrier systems," *IEEE Signal Processing Magazine*, Vol. 22, No. 6, pp. 108-122, 2005. Article (CrossRef Link)

[4] C. R. Johnson, P. Schniter, T. J. Endres, J. D. Behm, D. R. Brown and R. A. Casas, "Blind equalization using the constant modulus criterion: a review," in *Proc. of the IEEE*, Vol.86, No.10, pp.1927-1949, 1998. Article (CrossRef Link)

[5] T. Maksymyuk,L. Han,X. Ge,H. H. Chen,and M. Jo, "Quasi-quadrature Modulation Method for Power Efficient Video Transmission over LTE Networks," *IEEE Transactions on Vehicular Technology*, Vol. 63, No. 5, pp. 2083-2092, 2014. Article (CrossRef Link)

[6] J. Mai and A. H. Sayed, "A feedback approach to the steady-state performance of fractionally spaced blind adaptive equalizers," *IEEE Transactions on Signal Processing*, Vol. 48, No. 1, pp. 80-91, 2000. Article (CrossRef Link)

[7] F. C. C. De Castro, M. C. F. De Castro and D. S. Arantes, "Concurrent blind deconvolution for channel equalization," in *Proc. of the IEEE International Conference on Communications*, Helsinki, Finland, Vol.2, pp.366-371, 2001. Article (CrossRef Link)

[8] V. Weerackody and S. A. Kassam, "Dual-mode type algorithms for blind equalization," *IEEE Transactions on Communications*, Vol. 42, No. 1, pp. 22-28, 1994. Article (CrossRef Link)

[9] S. Chen, "Low complexity concurrent constant modulus algorithm and soft decision directed scheme for blind equalization," *IEE Proceedings-Vision Image and Signal Processing*, Vol. 150, No. 5, pp. 312-320, 2003. Article (CrossRef Link)

[10] N. Xie, H. Y. Hu, and H. Wang, "A new hybrid blind equalization algorithm with steady-state performance analysis," *Digital Signal Processing*, Vol. 22, No. 2, pp. 233-237, 2012. Article (CrossRef Link)

[11] M. T. M. Silva and J. Arenas-Garcia, "A soft-switching blind equalization scheme via convex combination of adaptive filters," *IEEE Transactions on Signal Processing*, Vol. 61, No. 5, pp. 1171-1182, 2013. Article (CrossRef Link)

[12] S. Barbarossa, A. Scaglione, "Blind equalization using cost function matched to the signal constellation," in *Proc. of 31st Asilomar Conference on Signals, Systems, Computers*, Pacific Grove, CA, USA, Vol. 1, pp. 550-554, 1997. Article (CrossRef Link)

[13] L. He, M. G. Amin, and C. Reed, "Adaptive equalization techniques for indoor dynamic wireless communication channels," in *Proc. of SPIE proceedings series*, Vol. 4395, No. 28, pp. 28-38, 2001. Article (CrossRef Link)

[14] L. He, M. G. Amin, C. Reed, Jr., and R. C. Malkemes, “A hybrid adaptive blind equalization algorithm for QAM signals in wireless communications,” *IEEE Transactions on Signal Processing*, Vol. 52, No. 7, pp. 2058-2069, 2004. Article (CrossRef Link)
[15] T. Thaiupathumpa, L. He, and S. A. Kassam, "Square contour algorithm for blind equalization of QAM signals," *Signal Processing*, Vol. 86, No. 11, pp. 3357-3370, 2006. Article (CrossRef Link)
[16] Y. Sato, "A method of self-recovering equalization for multilevel amplitude-modulation systems," *IEEE Transactions on Communications*, Vol. 23, No. 6, pp. 679-682, 1975. Article (CrossRef Link)
[17] L. He, S. A. Kassam, "Convergence analysis of blind equalization algorithms using constellation-matching," *IEEE Transactions on Communications*, Vol. 56, No. 11, pp. 1765-1768, 2008. Article (CrossRef Link)
[18] J. Yang, J. J. Werner, and G. A. Dumont, "The multimodulus blind equalization and its generalized algorithms," *IEEE Journal on Selected Areas in Communications*, Vol. 20, No. 5, pp. 997-1015, 2002. Article (CrossRef Link)
[19] S. A. Sheikh, P. Z. Fan, "New blind equalization techniques based on improved square contour algorithm," *Digital Signal Processing*, Vol. 18, No. 5, pp. 680-693, 2008. Article (CrossRef Link)
[20] S. Abrar, R. A. Axford Jr., "Sliced multi-modulus blind equalization algorithm," *ETRI journal*, Vol. 27, No. 3, pp. 257-266, 2005. Article (CrossRef Link)
[21] A. Labed, A. Aissa-El-Bey, T. Chonavel, and A. Belouchrani, "New hybrid adaptive blind equalization algorithms for QAM signals," in *Proc. of IEEE International Conference on Acoustics, Speech and Signal Processing*, Taipei, Taiwan, pp. 2809-2812, 2009. Article (CrossRef Link)
[22] X. L. Li, X. D. Zhang, "A family of generalized constant modulus algorithms for blind equalization," *IEEE Transactions on Communications*, Vol. 54, No. 11, pp. 1913-1917, 2006. Article (CrossRef Link)
[23] Y. Li, Z. Ding, "Global convergence of fractionally spaced Godard (CMA) adaptive equalizers," *IEEE Transactions on Signal Processing*, Vol. 44, No. 4, pp. 818-826, 1996. Article (CrossRef Link)
[24] B. Lin, R. He, X. Wang and B. Wang, "Excess MSE analysis of the concurrent constant modulus algorithm and soft decision-directed scheme for blind equalisation," *IET Signal Processing*, Vol. 2, No. 2, pp. 147-155, 2008. Article (CrossRef Link)
[25] A. Goupil and J. Palicot, "New algorithms for blind equalization: The constant norm algorithm family," *IEEE Transactions on Signal Processing*, Vol. 55, No. 4, pp. 1436–1444, 2007. Article (CrossRef Link)
[26] JM Filho, MD Miranda and MTM Silva, "A regional multimodulus algorithm for blind equalization of QAM signals: Introduction and steady-state analysis," *Signal Processing*, Vol. 92, No. 11, pp. 2643-2656, 2012. Article (CrossRef Link)
[27] V. Savaux, F. Bader, J. Palicot, "OFDM/OQAM Blind Equalization Using CNA Approach," *IEEE Transactions on Signal Processing*, Vol. 64, No. 9, pp. 2324–2333, 2016. Article (CrossRef Link)
[28] Marcelo A.C. Fernandes, "Linear programming applied to blind signal equalization," *AEU - International Journal of Electronics and Communications*, Vol. 69, No. 1, pp. 408-417, 2015. Article (CrossRef Link)

Wei Rao is an Associate Professor at Nanchang Institute of Technology, Nanchang, China. He received the B.E. and M.E. degrees from Anhui University of Science & Technology, Huainan, China, in 2003 and 2007, respectively. He is currently pursuing a doctoral degree at department of electronic engineering in Fudan University, Shanghai, China. His research interests include adaptive signal processing and wireless communication.

Changlong Lu received M.E. degree from Jingdezhen Ceramic Institute, Jingdezhen, China, in 2011. He is currently a Lecturer in department of electronic information engineering of Jingdezhen Ceramic Institute. His research interests include collaborative communications and internet of vehicles.

Yuanyuan Liu received the B.E. degree from NanChang University, NanChang, China, in 2005, the M.E. degree from Huazhong University of Science and Technology, Wuhan, China, in 2007, and the Ph.D. degree from Centrol China Normal University, Wuhan, China, in 2016. She is currently a Lecturer in China University of Geoscience. Her research interests include image processing, computer vision and pattern recognition.

Jian Qiu Zhang (M'98–SM'01) received the B.Sc. degree from East of China Institute of Engineering, Nanjing, in 1982, and the M.S. and Ph.D. degrees from Harbin Institute of Technology (HIT), Harbin, China, in 1992 and 1996, respectively. He is currently a Professor with the Department of Electronic Engineering, Fudan University, Shanghai, China. From 1999 to 2002, he was a Senior Research Fellow at the School of Engineering, University of Greenwich, Chatham Maritime, U.K. In 1998, he was a Visiting Research Scientist at the Institute of Intelligent Power Electronics, Helsinki University of Technology, Espoo, Finland. He was an Associate Professor from 1995 to 1997 and a Lecturer from 1989 to 1994 with the Department of Electrical Engineering, HIT. During 1982 to 1987, he was an Assistant Electronic Engineer at the 544th Factory, Hunan, China. His main research interests are signal processing and its application for advanced sensors, intelligent instrumentation systems and control, and communications.